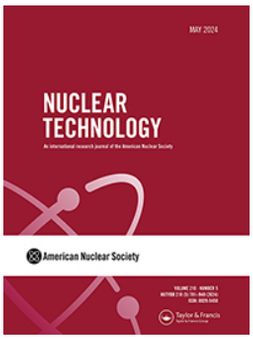

Nuclear Technology

ISSN: (Print) (Online) Journal homepage: www.tandfonline.com/journals/unct20

Construction of the Dynamic Model and Control System for the Canadian Supercritical Water–Cooled Reactor Power Plant

Huirui Han & Chao Zhang

To cite this article: Huirui Han & Chao Zhang (2024) Construction of the Dynamic Model and Control System for the Canadian Supercritical Water–Cooled Reactor Power Plant, Nuclear Technology, 210:5, 836-849, DOI: 10.1080/00295450.2023.2249710

To link to this article: https://doi.org/10.1080/00295450.2023.2249710

NUCLEAR TECHNOLOGY · VOLUME 210 · 836–849 · MAY 2024

DOI: https://doi.org/10.1080/00295450.2023.2249710

Construction of the Dynamic Model and Control System for the Canadian Supercritical Water–Cooled Reactor Power Plant

Huirui Han and Chao Zhang*

Western University, Department of Mechanical & Materials Engineering, 1151 Richmond Street, London, Ontario, N6A5B9, Canada

Received November 3, 2022
Accepted for Publication August 8, 2023

Abstract — *Canada has proposed the supercritical water–cooled reactor (SCWR) concept as one of the Generation IV nuclear reactors. In the SCWR power plant, the supercritical water is heated in the reactor and then flows to the turbine directly. Therefore, knowledge of the dynamic behaviors of the system is necessary for the stable operation of the power plant. There is still a lack of study on the control system for the proposed SCWR power plant. In this study, a dynamic model for the entire SCWR power plant is constructed that includes the reactor, turbine, condenser, and feedwater pump. Based on the model, the open-loop characteristics of the system when subjected to perturbations in the inputs are analyzed. Subsequently, a feedback control strategy is adopted to regulate the outputs of the system when there are disturbances. The evaluation of the performance of the control system shows that the proposed control system can return the plant back to the operating conditions effectively.*

Keywords — *Supercritical water–cooled reactor (SCWR), dynamic model, feedback control, control system, performance.*

Note — *Some figures may be in color only in the electronic version.*

I. INTRODUCTION

Interest in the nuclear power plant has increased in recent years due to increasing power demand and the adverse effects of climate change caused by fossil fuels. The supercritical water–cooled nuclear reactor (SCWR) was one of six concepts that have been proposed as Generation IV reactors.[1] Following the maturation of technologies in the existing light water–cooled reactors and supercritical fossil-fueled power plants, SCWRs have been under development in the past decade. The Canadian SCWR is a heavy water–moderated and supercritical light water–cooled reactor. To achieve a higher power conversion efficiency (>45%), it operates at 25 MPa. The fuel bundle in the reactor includes two-ring, 64-element fuel rods.[2]

In the SCWR power plant, the supercritical water is heated in the reactor and sent to the turbine directly. The heat balance between the reactor and the turbine is regulated by the pressure of the main steam since the temperature of the main steam needs to be kept constant in normal operation. If the reactor power is a little bit too high, the steam pressure will rise. In the nuclear power plant, two plant control strategies are mainly used: the reactor-following-turbine and the turbine-following-reactor operations.[3] In the reactor-following-turbine operation mode, the pressure of the main steam is controlled by the reactor while the turbine control valve regulates the electric power. In this operation mode, the reactor needs to respond rapidly to load changes. When the changes are sharp, the fluctuating flow rate of the steam may lead to considerable variations of temperatures in the reactor, such as the temperature of the cladding surface around the fuel rods, which will affect the safety of the reactor.

In the turbine-following-reactor mode, the pressure of the main steam is controlled by the turbine control valve and the electric power is controlled by the reactor power. The function of the turbine control valve is to

*E-mail: czhang@eng.uwo.ca

adjust the steam flow rate into the turbine. When the control valve opening is increased, the main steam flow rate increases, and then the pressure and the temperature of the main steam decrease. Although the response to load changes in this operation mode is slower than the former mode, the reactor power plant can run in relatively stable mode. Therefore, this operation mode is used in this work.

A few studies on the control system design for SCWR power plants have been conducted.[4–10] The turbine-following-reactor operation mode was used in the previous studies by Nakatsuka et al.[3,4] for the control system designs for the supercritical water–cooled fast reactor and the supercritical high-temperature thermal reactor power plant. Sun and Jiang[5] constructed a linear dynamic model for the Canada Deuterium Uranium (CANDU) SCWR system. Based on the linear dynamic model, the dynamic characteristics of the control system and the coupling analysis between different inputs and outputs of the system were presented.

Sun et al. and Sun and Jiang then attempted to use different control methods, such as the use of feedback controllers, feedforward controllers,[6,7] and the hybrid feedback and feedforward control strategy[8] to improve the performance of the control system. In addition, a linear parameter-varying strategy was also proposed by Sun et al.[9] to obtain satisfactory performance of the control system at different operating conditions. In these studies, the model of the reactor was simplified as a one-dimensional thermal system. However, the fluid flow and heat transfer in the power plant system are three dimensional. Therefore, the reactor model should be improved further based on the three-dimensional flow and heat transfer characteristics of the thermal system.

Maitri et al.[10] and Han et al.[11] proposed two-dimensional and three-dimensional models for the CANDU supercritical water–cooled reactor, respectively. Based on the 64-element SCWR (Ref. [2]), Han and Zhang[12] also proposed a linear dynamic model of the reactor that was constructed based on the full-scale three-dimensional computational fluid dynamics (CFD) simulations of the supercritical water flow and heat transfer in the rod channels.

In this study, the linear dynamic model of the 64-element Canadian SCWR power plant is first constructed. Based on the linear dynamic model, the dynamic responses of the outputs of the system when it is subjected to variations of the inputs are evaluated. Then, the feedback controllers are designed for the control system and the evaluation of the performance of the designed control system is carried out.

II. CONFIGURATION OF THE CANADIAN SCWR POWER PLANT

Figure 1 exhibits the diagram of the simplified Canadian SCWR power plant, and Table I shows the operating condition at the design point. The supercritical coolant goes into the fuel assembly in the reactor core. In the fuel assembly, the supercritical water flows downward through a central flow tube, and then reversely, upward through the fuel elements in the fuel bundle. After the water absorbs the heat generated by nuclear fission in the fuel rods, it flows

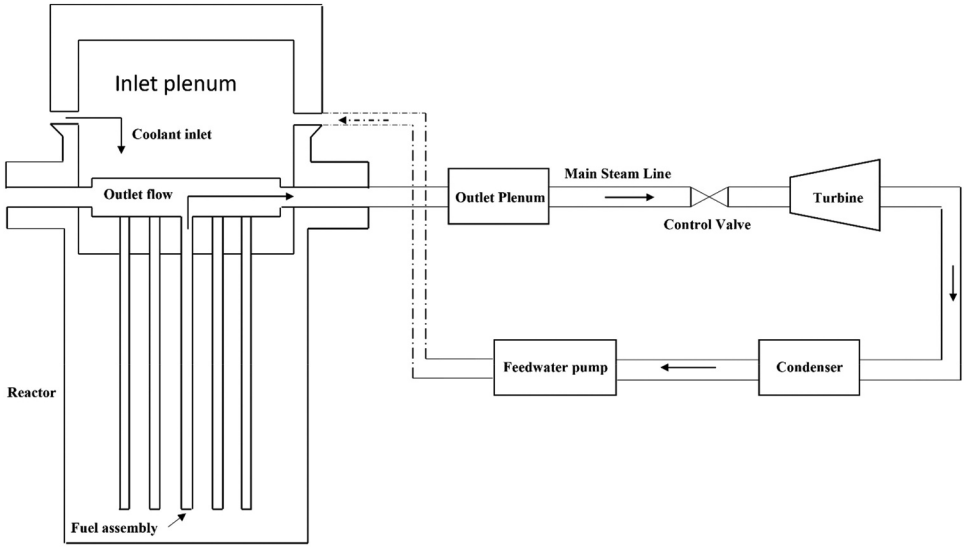

Fig. 1. Diagram of the Canadian SCWR power plant.

TABLE I

Specifications of the Canadian SCWR

Thermal power	2540 MW
Flow rate	1320 kg/s
Number of channels	336
Inlet temperature	350°C
Operating pressure	25 MPa
Heated length	5 m

into the turbine through the outlet header. After the turbine, the working fluid flows into the condenser. Then the feedwater from the condenser is pumped back to the reactor, as shown in Fig. 1. In order to operate the reactor in a relatively stable mode, the control strategy used in this study is the turbine-following-reactor operation. The main steam from the nuclear reactor drives the turbine, and the control valve of the turbine is used to adjust the main steam flow rate going into the turbine and to keep the pressure of the main steam as the design point.

III. CONSTRUCTION OF THE DYNAMIC MODEL FOR THE CANADIAN SCWR POWER PLANT

In order to construct the dynamic model for the SCWR power plant, dynamic models are needed for all components in the SCWR power plant.

III.A. Linear Dynamic Models for Each Component

III.A.1. Feedwater Pump

The transfer function of the dynamic model of the feedwater pump can be expressed as[5]

$$G_{FP,P(s)} = \frac{\delta M_{FP,P(s)}}{\delta P_{C(s)}} = -39.6 \quad , \tag{1}$$

where $M_{FP,P}$ is the change in the mass flow rate of the feedwater contributed by the pressure of the condenser P_C.

III.A.2. Reactor

The dynamic model for the reactor consists of three inputs, which are the inlet coolant mass flow rate, the inlet coolant temperature, and the heat input, and three outputs, which are the outlet coolant mass flow rate, the outlet coolant temperature, and the maximum wall temperature. The transient full-scale three-dimensional CFD simulations are used to construct the linear dynamic model for the reactor. A 10% step perturbation for one input is added to the steady state, and the resulting changes of all three outputs are obtained through transient CFD simulations. This process is repeated for every input variable. Thus, the recorded responses would consist of nine pairs of input and output.

From these data sets, the least-squares method–based system identification technique[13] is used to choose the best fitting for the dynamic models. The parameters of the dynamic models are determined by minimizing the sum of the squares of differences between the results from CFD simulations and the outputs from the dynamic models. The responses from the linear dynamic model are verified with the results from transient CFD simulations, which shows that the linear dynamic model can capture the transient behavior in the reactor. More details on the CFD simulations and the development of the linear dynamic model based on the CFD results are given in Ref. [12].

The transfer functions of the linear dynamic models for the reactor in the Laplace form are shown as[12]

$$G_{R(s)} = \begin{bmatrix} \frac{\delta M_{R(s)}}{\delta M_{FP(s)}} & \frac{\delta M_{R(s)}}{\delta T_{in(s)}} & \frac{\delta M_{R(s)}}{\delta q_{(s)}} \\ \frac{\delta T_{R(s)}}{\delta M_{FP(s)}} & \frac{\delta T_{R(s)}}{\delta T_{in(s)}} & \frac{\delta T_{R(s)}}{\delta q_{(s)}} \\ \frac{\delta T_{W\_max(s)}}{\delta M_{FP(s)}} & \frac{\delta T_{W\_max(s)}}{\delta T_{in(s)}} & \frac{\delta T_{W\_max(s)}}{\delta q_{(s)}} \end{bmatrix} , \tag{2}$$

$$\frac{\delta M_{R(s)}}{\delta M_{FP(s)}} = \frac{42.95s^2 + 52.54s + 44.28}{s^3 + 68.48s^2 + 96.16s + 44.29} \quad , \tag{3}$$

$$\frac{\delta M_{R(s)}}{\delta T_{in(s)}} = \frac{0.01139s^5 + 0.02959s^4 + 0.1029s^3 + 0.1088s^2 + 0.1427s + 0.03218}{s^5 + 2.707s^4 + 8.535s^3 + 10.62s^2 + 10.94s + 3.182} \quad , \tag{4}$$

$$\frac{\delta M_{R(s)}}{\delta q_{(s)}} = \frac{\begin{array}{c} 0.0004862s^8 + 0.002397s^7 + 0.03164s^6 + 0.1042s^5 \\ + 0.5411s^4 + 1.088s^3 + 2.705s^2 + 2.906s + 1.057 \end{array}}{\begin{array}{c} s^9 + 262.7s^8 + 1501s^7 + 1.655 \times 10^4 s^6 + 5.982 \times 10^4 s^5 + 2.491 \times 10^5 s^4 \\ + 4.864 \times 10^5 s^3 + 8.496 \times 10^5 s^2 + 7.166 \times 10^5 s + 2.13 \times 10^5 \end{array}} \quad , \tag{5}$$

$$\frac{\delta T_{R(s)}}{\delta M_{FP(s)}} = \frac{-35.43s^6 - 50.78s^5 - 797.6s^4 - 170s^3 - 1537s^2 + 5183s + 3600}{s^7 + 4.627s^6 + 30.51s^5 + 92.96s^4 + 175.4s^3 + 202.8s^2 + 53.42s + 22.47} \quad , \tag{6}$$

$$\frac{\delta T_{R(s)}}{\delta T_{in(s)}} = \frac{\begin{array}{l} 166.2s^{15} + 6078s^{14} + 1.071\times10^4 s^{13} + 3.949\times10^5 s^{12} + 1.82\times10^5 s^{11} + 7.999\times10^6 s^{10} \\ +9.215\times10^5 s^9 + 6.96\times10^7 s^8 - 1.624\times10^6 s^7 + 2.763\times10^8 s^6 - 2.191\times10^7 s^5 \\ +4.669\times10^8 s^4 - 4.11\times10^7 s^3 + 2.655\times10^8 s^2 - 1.392\times10^7 s + 2.132\times10^7 \end{array}}{\begin{array}{l} s^{19} + 13.11s^{18} + 179.1s^{17} + 1429s^{16} + 1.043\times10^4 s^{15} + 5.761\times10^4 s^{14} + 2.716\times10^5 s^{13} \\ +1.101\times10^6 s^{12} + 3.575\times10^6 s^{11} + 1.11\times10^7 s^{10} + 2.46\times10^7 s^9 + 6.09\times10^7 s^8 + 8.591\times10^7 s^7 + 1.767\times10^8 s^6 \\ +1.376\times10^8 s^5 + 2.429\times10^8 s^4 + 7.938\times10^7 s^3 + 1.215\times10^8 s^2 + 6.714\times10^6 s + 9.625\times10^6 \end{array}} \quad , \tag{7}$$

$$\frac{\delta T_{R(s)}}{\delta q_{(s)}} = \frac{10^{-4}\left(2.576\ s^3 + 6.862s^2 + 4.012s + 2.553\right)}{s^4 + 2.373s^3 + 2.146s^2 + 1.093s + 0.299} \quad , \tag{8}$$

$$\frac{\delta T_{W\_max(s)}}{\delta M_{FP(s)}} = \frac{20.46s^4 + 281.9s^3 + 448.8s^2 + 909.5s + 211.8}{s^5 + 1.76s^4 + 5.969s^3 + 6.427s^2 + 4.194s + 1.101} \quad , \tag{9}$$

$$\frac{\delta T_{W\_max(s)}}{\delta T_{in(s)}} = \frac{-3.388s^8 - 10.24s^7 - 162.5s^6 - 404.6s^5 - 1601s^4 - 2369s^3 - 977s^2 - 640.5s + 53.52}{s^9 + 1.862s^8 + 55.11s^7 + 80.76s^6 + 674s^5 + 588.6s^4 + 1118s^3 + 670.3s^2 + 389.8s + 9.111} \quad , \tag{10}$$

$$\frac{\delta T_{W\_max(s)}}{\delta q_{(s)}} = \frac{10^{-4}\ (73.78s + 7.294)}{s^6 + 4.655s^5 + 15.79s^4 + 20.64s^3 + 14.44s^2 + 7.749s + 0.7372} \quad . \tag{11}$$

The details on the validation of the linear dynamic models of Eqs. (3), (7), and (11) are shown in the Appendix.

III.A.3. Outlet Plenum

The outlet plenum in this study consisted of the outlet feeders and the outlet header. A total of 336 fuel channels were assembled in the reactor. Therefore, 336 outlet feeders connect the reactor to one outlet header. The transfer function of the outlet plenum is given as[5]

$$G_{OP(s)} = \begin{bmatrix} \frac{\delta T_{OP(s)}}{\delta T_{R(s)}} & \frac{\delta T_{OP(s)}}{\delta M_{R(s)}} \\ \frac{\delta M_{OP(s)}}{\delta T_{R(s)}} & \frac{\delta M_{OP(s)}}{\delta M_{R(s)}} \end{bmatrix} = \begin{bmatrix} \frac{3.2292}{(s+0.69)(s+4.68)} & 0 \\ \frac{1.14s^2 + 0.7866s + 0.034866}{(s+0.69)(s+4.68)} & 336 \end{bmatrix} \quad , \tag{12}$$

where T_{OP} and M_{OP} are outlet temperature and outlet mass flow rate of the outlet plenum, respectively.

III.A.4. Main Steam Line

The main steam line connects the reactor and the turbine; therefore, the variations of the temperature and the mass flow rate of the outlet plenum in the reactor will affect the temperature and the pressure of the main steam line. The transfer function of the main steam line between the reactor and turbine is shown as[5]

$$G_{MSL(s)} = \begin{bmatrix} \frac{\delta T_{MSL(s)}}{\delta T_{OP(s)}} & \frac{\delta T_{MSL(s)}}{\delta M_{OP(s)}} & \frac{\delta T_{MSL(s)}}{\delta M_{MSL(s)}} \\ \frac{\delta P_{MSL(s)}}{\delta T_{OP(s)}} & \frac{\delta P_{MSL(s)}}{\delta M_{OP(s)}} & \frac{\delta P_{MSL(s)}}{\delta M_{MSL(s)}} \end{bmatrix} = \begin{bmatrix} \frac{0.7}{s+0.7} & 0 & 0 \\ \frac{3\times10^{-2}}{s+0.7} & \frac{1.31\times10^{-2}}{s} & -\frac{1.31\times10^{-2}}{s} \end{bmatrix}, \quad (13)$$

where T_{MSL} and P_{MSL} are the temperature and pressure of the main steam, respectively.

III.A.5. Turbine Control Valve

When the heat in the reactor is a bit too high, the pressure of the main steam will go up. In the turbine-following-reactor control strategy, the opening of the control valve needs to be larger to increase the main steam flow rate so that the pressure of main steam can be regulated back to the design point. The transfer function of the control valve is described as[5]

$$G_{CV(s)} = \begin{bmatrix} \frac{\delta M_{MSL(s)}}{\delta A_{CV(s)}} & \frac{\delta M_{MSL(s)}}{\delta T_{MSL(s)}} & \frac{\delta M_{MSL(s)}}{\delta P_{MSL(s)}} \end{bmatrix} = \begin{cases} [2640 \quad -0.37 \quad 26.74] & A_{CV} \le 50\% \\ [792 \quad -0.37 \quad 26.74] & A_{CV} > 50\% \end{cases}, \quad (14)$$

where A_{CV} is the percentage of the control valve opening and M_{MSL} is the mass flow rate of the main steam, respectively.

III.A.6. Turbine and Condenser

In this study, we assumed the pressure in the condenser is constant. The transfer functions of the turbine and condenser are given as[14]

$$G_{T(s)} = \left[\frac{\delta P_{T(s)}}{\delta P_{MSL(s)}}\right] = \left[2.68\times10^{-4}\right] \quad (15)$$

$$G_{C(s)} = \left[\frac{\delta P_{C(s)}}{\delta P_{T(s)}}\right] = [1], \quad (16)$$

where P_T and P_C are the pressures of the turbine and the condenser, respectively.

III.B. Linear Dynamic Model for the SCWR Power Plant

The block diagram of the linear dynamic model for the Canadian SCWR power plant is shown in Fig. 2. The inputs of the dynamic model are the feedwater flow rate, the heat flux on the fuel rod, and the opening percentage of the control valve. The outputs of the dynamic model are the outlet temperature of the outlet plenum, the maximum wall temperature of the fuel rods, and the pressure of the main steam (Fig. 2).

The relationship between the inputs and outputs of the Canadian SCWR power plant is

$$\begin{bmatrix} \delta T_{OP} \\ \delta T_{W\_max} \\ P_{MSL} \end{bmatrix} = \begin{bmatrix} G_{11} & G_{12} & G_{13} \\ G_{21} & G_{22} & G_{23} \\ G_{31} & G_{32} & G_{33} \end{bmatrix} \begin{bmatrix} \delta M_{FP} \\ \delta q \\ \delta A_{CV} \end{bmatrix}, \quad (17)$$

where the transfer functions of the linear dynamic model are presented in the following:

$$G_{11} = \frac{-35.43s^6 - 50.78s^5 - 797.6s^4 - 170s^3 - 1537s^2 + 5183s + 3600}{s^7 + 4.627s^6 + 30.51s^5 + 92.96s^4 + 175.4s^3 + 202.8s^2 + 53.42s + 22.47}, \quad (18)$$

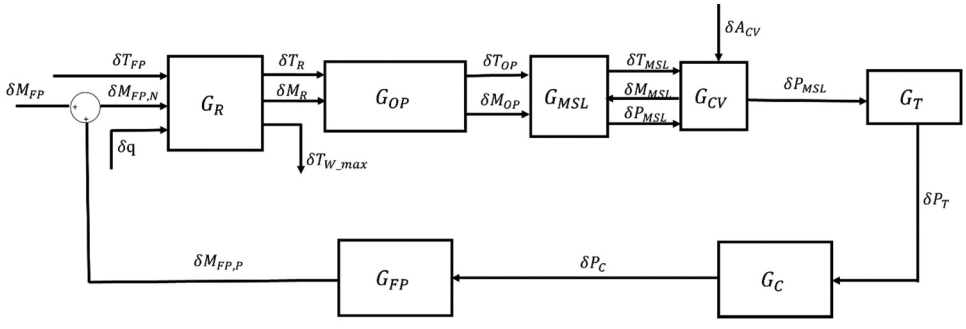

Fig. 2. Block diagram of the linear dynamic model for the Canadian SCWR power plant.

$$G_{12} = \frac{10^{-4}\left(8.318s^3 + 22.16s^2 + 12.96s + 8.244\right)}{s^6 + 7.743s^5 + 18.12s^4 + 20.28s^3 + 13.1s^2 + 5.135s + 0.9655} \quad , \tag{19}$$

$$G_{13} = 0 \quad , \tag{20}$$

$$G_{21} = \frac{20.46s^4 + 281.9s^3 + 448.8s^2 + 909.5s + 211.8}{s^5 + 1.76s^4 + 5.969s^3 + 6.427s^2 + 4.194s + 1.101} \quad , \tag{21}$$

$$G_{22} = \frac{7.378 \times 10^{-3}s + 7.294 \times 10^{-4}}{s^6 + 4.655s^5 + 15.79s^4 + 20.64s^3 + 14.44s^2 + 7.749s + 0.7372} \quad , \tag{22}$$

$$G_{23} = 0 \quad , \tag{23}$$

$$G_{31} = \frac{0.9309s^2 + 1.139s + 0.9595}{s^3 + 68.48s^2 + 96.16s + 44.29} \quad , \tag{24}$$

$$G_{32} = 0 \quad , \tag{25}$$

$$G_{33} = \frac{\begin{array}{c}-34.45s^{13} - 742s^{12} - 6111s^{11} - 2.432 \times 10^4 s^{10} - 4.924 \times 10^4 s^9 - 5.107 \times 10^4 s^8 \\ -2.815 \times 10^4 s^7 - 8546s^6 - 1530s^5 - 163.8s^4 - 10.05s^3 - 0.3163s^2 - 3.854 \times 10^{-3}s - 2.145 \times 10^{-6}\end{array}}{\begin{array}{c}s^{14} + 22.22s^{13} + 194.4s^{12} + 856.7s^{11} + 2043s^{10} + 2711s^9 + 2068s^8 + 974.2s^7 \\ +276s^6 + 48.01s^5 + 5.096s^4 + 0.3125s^3 + 9.872 \times 10^{-3}s^2 + 1.21 \times 10^{-4}s + 6.755 \times 10^{-8}\end{array}} \quad . \tag{26}$$

IV. EVALUATION OF THE DYNAMIC MODEL FOR CANADIAN SCWR POWER PLANT

IV.A. Dynamic Characteristics of the Open-Loop System

In order to capture the dynamic behaviors of the system when it is subjected to disturbances, the output responses were obtained when a ±5% step perturbation was added at each input and the other two inputs were held at the design point values. Figures 3, 4, and 5 present the changes of the three outputs of the system due to the disturbances of the inputs, respectively. The dynamic responses of the open loop subjected to disturbances are summarized in Table II.

IV.A.1. Step Increase in the Feedwater Flow Rate

The heat flux and the control valve opening were kept unchanged when a 5% step decrease was added in the feedwater flow rate. From Figs. 3, 4, and 5, it can be seen that due to the increase in the feedwater flow rate, the temperature of the outlet plenum and the maximum wall temperature decreased. At steady state, the decrease magnitudes were 26.4°C (3.6%) and 31.6°C (3.4%), respectively, while the main steam pressure increased by 0.36 MPa (1.44%).

IV.A.2. Step Decrease in the Heat Flux

A 5% step decrease in the heat flux on the fuel rod was introduced. At the same time, the feedwater flow rate and the control valve opening remained at the design values. Figures 3, 4, and 5 show that the step decrease of the heat flux resulted in an 18.8°C drop in the temperature of the outlet plenum and a 43.6°C drop in the maximum wall temperature at steady state, but had almost no impact on the main steam pressure.

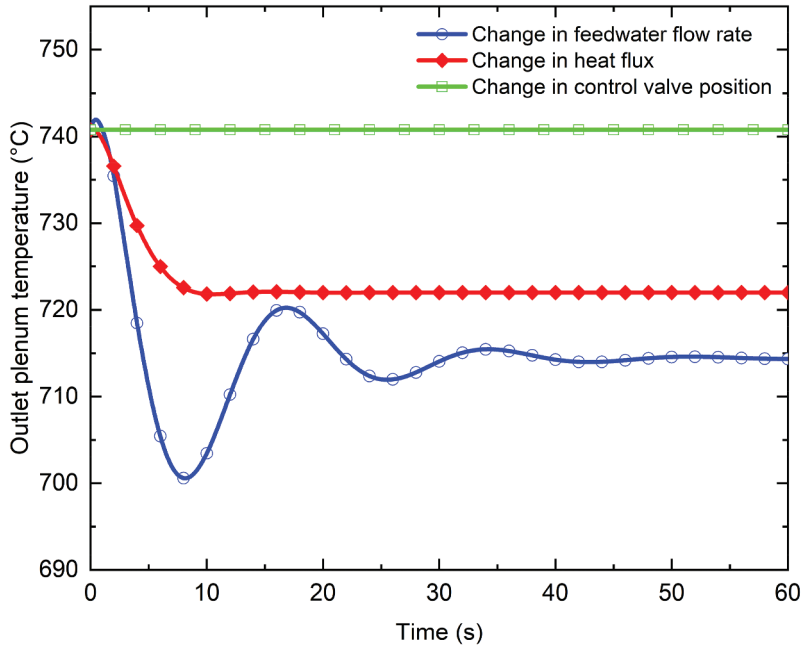

Fig. 3. Responses of the temperature of the outlet plenum to step variations of different inputs.

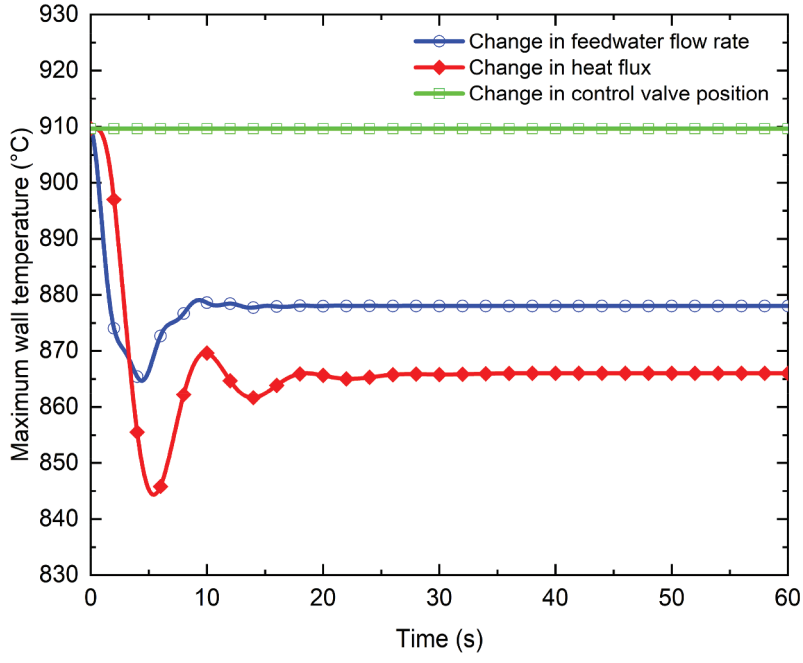

Fig. 4. Responses of the maximum wall temperature of fuel rods to step variations of different inputs.

IV.A.3. Step Decrease in the Control Valve Opening

The control valve opening reduced by 5% when the feedwater flow rate and the heat flux remained unchanged. It is shown that the main steam pressure rose by 0.8 MPa at steady state due to the step decrease in the control valve opening. In addition, the temperature of the outlet plenum and the maximum wall temperature were not affected by the change in the control valve opening.

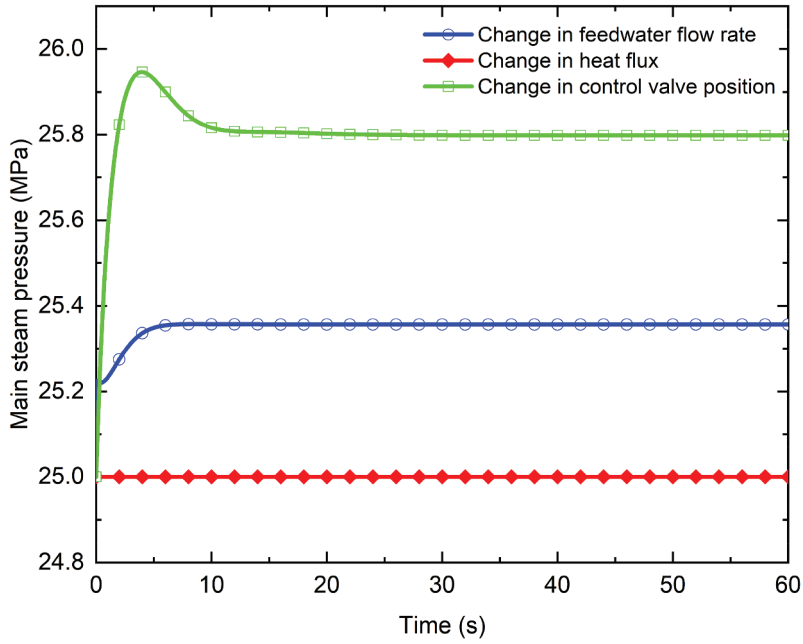

Fig. 5. Responses of the pressure of the main steam line to step variations of different inputs.

TABLE II

Summary of Quantitative Dynamics of the Open Loop

Disturbances	Overshoot (%) and Settling Time (s)		
	Outlet Plenum Temperature	Maximum Wall Temperature	Main Steam Pressure
M_{FP}: +5% q: −5% A_{CV}: −5%	−3.6 (41) −2.97 (10) 0 (0)	−3.4 (9.8) −4.79 (18.1) 0 (0)	1.44 (5.3) 0 (0) 3.2 (7.8)

IV.B. Cross Coupling of Inputs and Outputs

The coupling degree between the different inputs and outputs of the Canadian SCWR power plant at steady state was determined so that the most relevant input and output could be paired before the design of the controllers. The relative gain array (RGA) is commonly used to evaluate the cross coupling between inputs and outputs of a system at the steady-state condition.[15,16] It is used for evaluating the influence of an input on an output with respect to that on the rest of the outputs. All elements in a row/column sum to unity in the RGA. Elements with relative gains near 1 should be paired, and elements with negative relative gains should not be paired for control.[16] The steady-state gain matrix K of the entire SCWR system is the ratio of the amplitude of the output and the input in steady state (s = 0), which is calculated as

$$\mathrm{K} = \begin{bmatrix} 160.23 & 9 \times 10^{-4} & 0 \\ 192.29 & 10^{-3} & 0 \\ 0.02 & 0 & -31.75 \end{bmatrix} . \quad (27)$$

Based on K, the RGA of the system is calculated as

$$\mathrm{RGA} = \begin{bmatrix} 1.49 & -0.49 & 0 \\ -0.49 & 1.49 & 0 \\ 0 & 0 & 1 \end{bmatrix} . \quad (28)$$

It is obvious that the diagonal inputs and outputs are dominantly paired. The system can be regarded as diagonally dominant and a multiple single-input single-output

system at the design operating condition. Therefore, the outlet temperature of the outlet plenum is controlled by the mass flow rate of the feedwater, the maximum cladding temperature is regulated by the heat flux on the fuel rod, and the pressure of the main steam pressure is adjusted by the opening percentage of the control valve.

V. DESIGN AND PERFORMANCE EVALUATION OF THE FEEDBACK CONTROL SYSTEM

V.A. Design of the Feedback Control System

In the feedback control system, the controllers are used for regulating the deviations of the corresponding outputs to zero or as small as possible when the system is subjected to disturbances. Therefore, three controllers are needed for this three-input and three-output system. The general transfer function for a proportional-integral-derivative (PID) controller is expressed as[17]

$$C_{(s)} = K_P + K_I/s + K_D s \quad , \tag{29}$$

where K_P, K_I, and K_D are the proportional, integral, and derivative gains, respectively. The parameters of the controllers are tuned to meet the control requirements for the system[3,6]: (1) the overshoot is less than 15%, (2) the rise time is less than 20s, and (3) the settling time is below 50s. Table III shows the parameters for the controllers used in the feedback control system.

TABLE III
Parameters and Specifications of the Controllers

Controllers	K_P	K_I	K_D	Rising Time (s)	Settling Time (s)	Overshoot (%)
PID_1	0.0026	7.8608E–4	0.0022	17.5	43.7	0
I_2		150.0763		4.91	26.3	0
PI_3	−0.0599	−0.088		0.736	2.72	5.88

V.B. Performance Evaluation of the Control System

In order to evaluate the performance of the designed feedback control system, the deviations of the outputs from the design point due to the 5% step perturbations on the inputs were evaluated, and the controllers were activated to regulate the outputs of the system back to the design point. T = 0 is the time when the controllers were activated. The responses of the outlet plenum temperature, the maximum wall temperature, and the main steam pressure after the controllers were activated are shown in Figs. 6, 7, and 8, respectively.

It can be seen that the outlet plenum temperature and the maximum wall temperature increase and settle at the original design values in 50s using the feedback control system, as shown in Figs. 6 and 7, respectively. The response of the control system to a 0.8-MPa step increase in the main steam pressure is presented in Fig. 8, which shows that the main steam pressure can rapidly go back

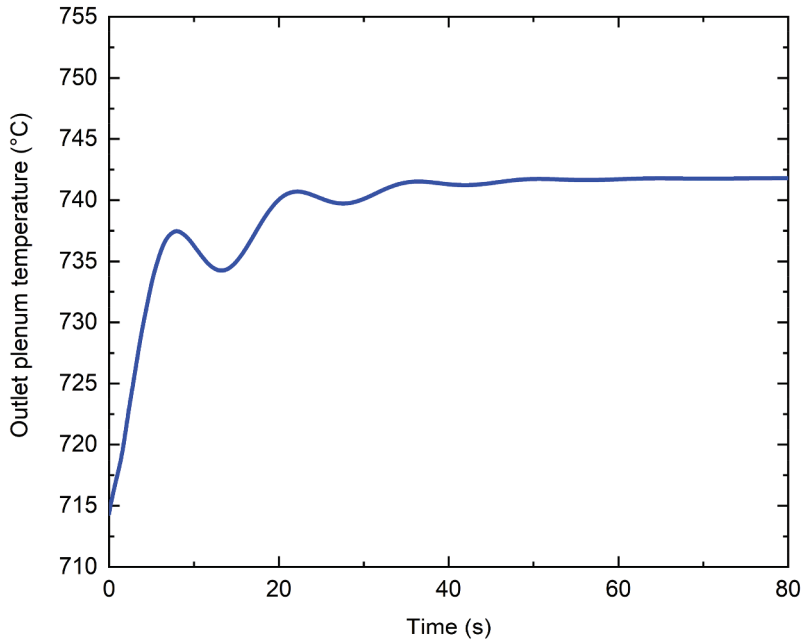

Fig. 6. Response of the temperature of the outlet plenum using the feedback control after the step perturbation was introduced.

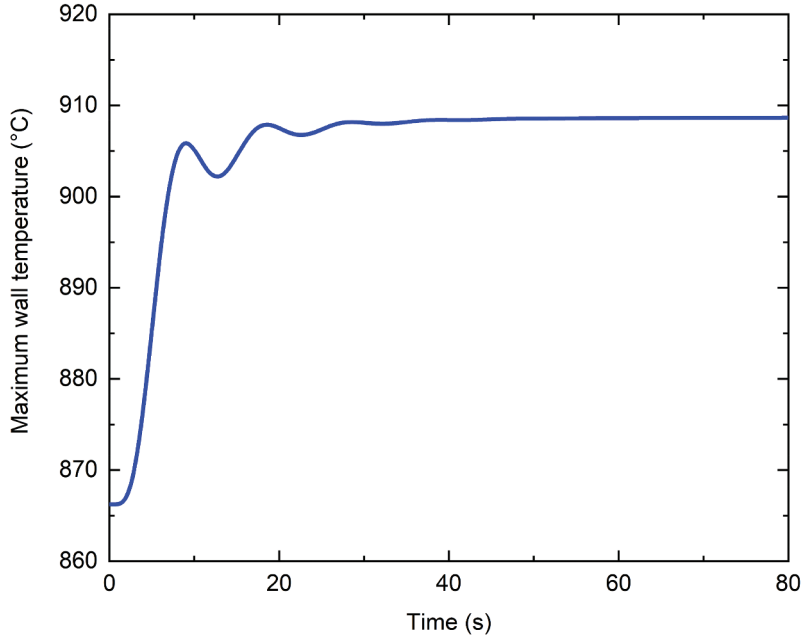

Fig. 7. Response of the maximum wall temperature of fuel rods using the feedback control after the step perturbation was introduced.

to the design value. In general, the feedback control system can return the system back to the design point in around 50s. Therefore, the designed feedback control system can effectively regulate and return the power plant back to the design point when there are perturbations.

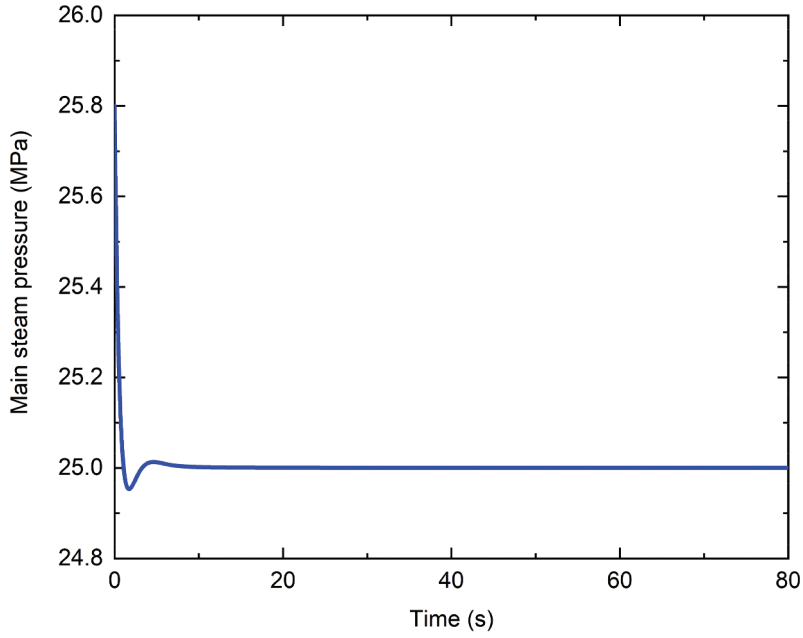

Fig. 8. Response of the pressure of the main steam using the feedback control after the step perturbation was introduced.

VI. CONCLUSION

The construction of the linear dynamic model and feedback control system for the Canadian SCWR power plant, which focus on the thermodynamic aspect, were developed in this study. Based on the linear dynamic model, the dynamic responses of the outputs of the system were investigated when the perturbations of input variables were introduced. Three controllers were designed in the feedback control system to reduce the deviations of the outputs to zero.

The performance of the feedback control system was also evaluated. The results show that the designed control system can regulate the system to the designed operating condition satisfactorily. Since 10% step disturbances were used to construct the linear dynamic models, the applicability of using transfer functions in the proposed control system is within 10% of the design point.

APPENDIX

In this work, CFD simulations were used to obtain the results of the nonlinear fluid flow and heat transfer process in the reactor since experimental data are not available now. The fluid flow and heat transfer process is governed by conservation equations of mass, momentum, and energy. The Reynolds-averaged form of these equations are given as follows[16]

$$\frac{\partial \rho}{\partial t} + \frac{\partial \rho \overline{u_i}}{\partial x_i} = 0 \quad ,$$

$$\frac{\partial \rho \overline{u_i}}{\partial t} + \frac{\partial \left(\rho \overline{u_i u_j}\right)}{\partial x_j} = -\frac{\partial \overline{p}}{\partial x_i} + \frac{\partial}{\partial x_j}\left(\mu \frac{\partial \overline{u_i}}{\partial x_j} - \rho \overline{u_i' u_j'}\right) + \rho g_i \quad ,$$

$$\frac{\partial \left(\rho c_p T\right)}{\partial t} + \frac{\partial}{\partial x_i}\left(\overline{u_i'} \rho c_p T\right) = \frac{\partial}{\partial x_i}\left[\left(\lambda + \frac{c_p \mu_t}{Pr_t}\right)\frac{\partial T}{\partial x_i}\right] \quad .$$

For the dynamic model of Eq. (3), a +10% step perturbation of the inlet mass flow rate was added, while the inlet temperature and the heat flux were kept unchanged. For the dynamic model of Eq. (7), a −10% step perturbation of the inlet temperature was added, while the inlet mass flow rate and the heat flux were kept unchanged. For the dynamic model of Eq. (11), a −10% step perturbation of the heat flux was added, while the inlet mass flow rate and the inlet temperature were kept unchanged.

The resulting changes of the outputs were all obtained though transient CFD simulations. Based on the relationships of the respective inputs and outputs, the transfer functions for these linear dynamic models were constructed to represent the linear time-invariant system. The parameters of models were regulated to minimize the sum of the squares of differences between the outputs from the dynamic models and the results from the CFD simulations. Comparisons are presented in Figs. A.1, A.2, and A.3.

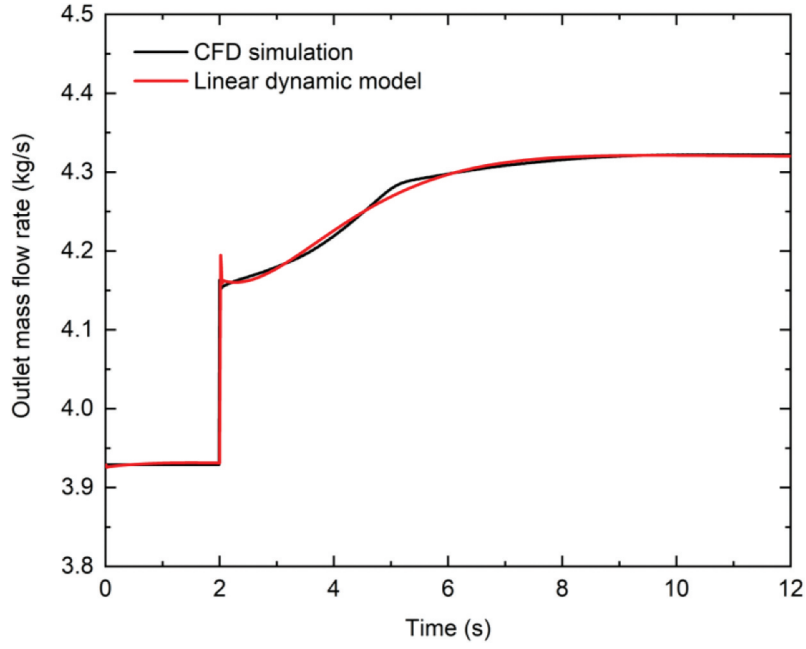

Fig. A.1. Validation for Eq. (3).

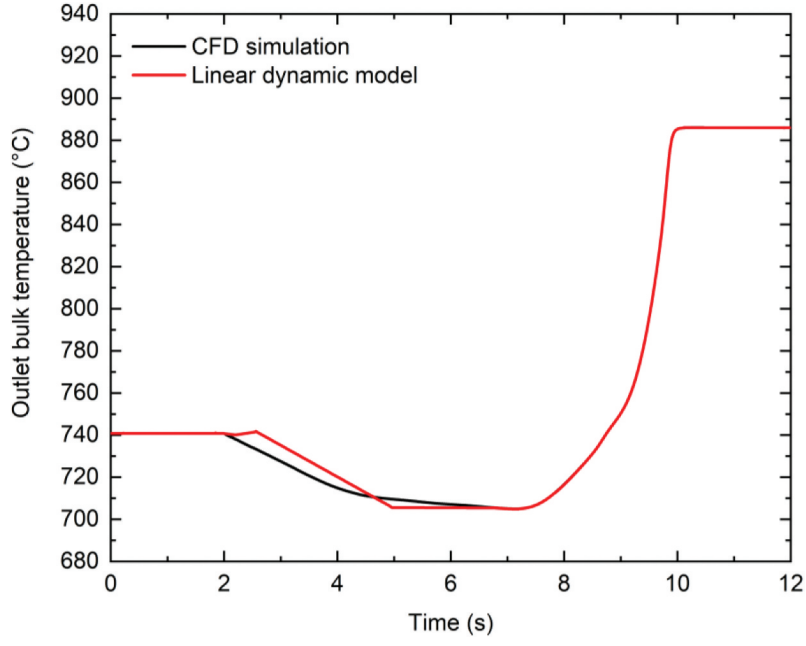

Fig. A.2. Validation for Eq. (7).

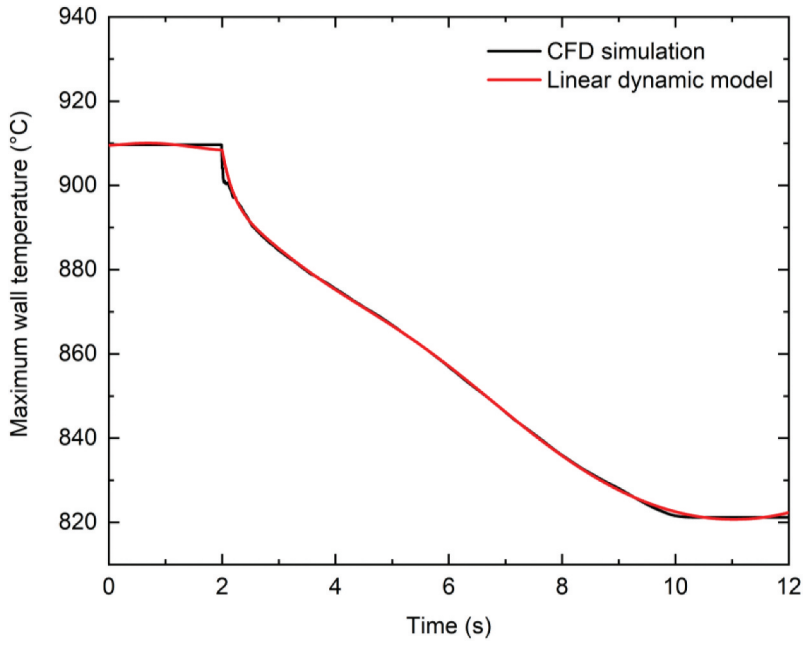

Fig. A.3. Validation for Eq. (11).

Nomenclature

A_{CV} = percentage of the control valve opening, %
G = transfer function
G_{11} = transfer function from the outlet plenum temperature to the feedwater flow rate
G_{12} = transfer function from the outlet plenum temperature to the heat flux
G_{13} = transfer function from the outlet plenum temperature to the control valve opening
G_{21} = transfer function from the maximum wall temperature to the feedwater flow rate
G_{22} = transfer function from the maximum wall temperature to the heat flux
G_{23} = transfer function from the maximum wall temperature to control valve opening
G_{31} = transfer function from the main steam pressure to the feedwater flow rate
G_{32} = transfer function from the main steam pressure to the heat flux
G_{33} = transfer function from the main steam pressure to the control valve opening
K_D = derivative gain
K_I = integral gain
K_P = proportional gain
M = mass flow rate (kg/s)
P = pressure (Pa)
q = heat flux (W/m^2)
s = complex variable in Laplace transform
T = temperature (^{o}C)

Subscripts

c = condenser
CV = control valve
FP = feedwater pump
MSL = main steam line
OP = outlet plenum
in = inlet
R = reactor
T = turbine
W = wall
max = maximum

Acronyms

CANDU: Canada Deuterium Uranium
CFD: computational fluid dynamics

RGA: relative gain array

SCWR: supercritical water–cooled reactor

Disclosure Statement

No potential conflict of interest was reported by the authors.

Funding

This work was supported by NSERC.

ORCID

Huirui Han http://orcid.org/0000-0001-9475-6957

References

1. "R&D Outlook for Generation IV Nuclear Energy Systems: 2018 Update," Gen IV International Forum (2018).
2. M. YETISIR et al., "Fuel Assembly Concept of the Canadian Supercritical Water-Cooled Reactor," *J. Nucl. Eng. Radiat. Sci*, **4**, *1*, 1 (Jan. 2018); https://doi.org/10.1115/1.4037818.
3. T. NAKATSUKA, Y. OKA, and S. KOSHIZUKA, "Control of a Fast Reactor Cooled by Supercritical Light Water," *Nucl. Technol.*, **121**, *1*, 81 (Jan. 1998); https://doi.org/10.13182/NT98-A2821.
4. Y. ISHIWATARI, Y. OKA, and S. KOSHIZUKA, "Control of a High Temperature Supercritical Pressure Light Water Cooled and Moderated Reactor with Water Rods," *J. Nucl. Sci. Technol.*, **40**, *5*, 298 (May 2003).
5. P. SUN and J. JIANG, "Construction and Analysis of a Dynamic Model for a Canadian Direct-Cycle SCWR for Control System Studies," *Nucl. Technol.*, **180**, *3*, 399 (2012); https://doi.org/10.13182/NT12-A15352.
6. P. SUN et al., "Control of Canadian Once-Through Direct Cycle Supercritical Water-Cooled Reactors," *Ann. Nucl. Energy*, **81**, 6 (July 2015); https://doi.org/10.1016/j.anucene.2015.03.008.
7. P. SUN and J. ZHANG, "Control Strategy Study for Once-Through Direct Cycle Canadian SCWRs," *Prog. Nucl. Energy*, **98**, 202 (July 2017); https://doi.org/10.1016/j.pnucene.2017.03.024.
8. P. SUN et al., "Robust Control of Once-Through Canadian Supercritical Water-Cooled Reactors," *Nucl. Technol.*, **199**, *1*, 35 (2017); https://doi.org/10.1080/00295450.2017.1322396.
9. P. SUN, J. ZHANG, and G. SU, "Linear Parameter-Varying Modeling and Control of the Steam Temperature in a Canadian SCWR," *Nucl. Eng. Des.*, **313**, 225 (Mar. 2017); https://doi.org/10.1016/j.nucengdes.2016.12.025.
10. R. V. MAITRI, C. ZHANG, and J. JIANG, "Computational Fluid Dynamic Assisted Control System Design Methodology Using System Identification Technique for CANDU Supercritical Water Cooled Reactor (SCWR)," *Appl. Therm. Eng.*, **118**, 17 (2017); https://doi.org/10.1016/j.applthermaleng.2017.02.079.
11. H. HAN, C. ZHANG, and J. JIANG, "Dynamic Models and Control System Design for Heated Channels in a Canadian SCWR," *Ann. Nucl. Energy*, **151**, 107973 (Feb. 2021); https://doi.org/10.1016/j.anucene.2020.107973.
12. H. HAN and C. ZHANG, "Construction of a Feedback Control System Based on CFD Simulations for the 64-Element Canadian SCWR," *Prog. Nucl. Energy*, **164**, 104894 (2023); https://doi.org/10.1016/j.pnucene.2023.104894.
13. L. LJUNG, "System Identification Toolbox: User's Guide, R2022a," The MathWorks, Inc. (2015).
14. B. CUI, "3keymaster SCWR Simulator Graph," CIES Laboratory (2016).
15. E. BRISTOL, "On a New Measure of Interaction for Multivariable Process Control," *IEEE Trans. Automat. Contr.*, **11**, *1*, 133 (Jan. 1966); https://ieeexplore.ieee.org/document/1098266.
16. S. SKOGESTAD and I. POSTLETHWAITE, *Multivariable Feedback Control: Analysis and Design*, 2nd ed., John Wiley, Chichester, England (2005).
17. N. S. NISE, *Control Systems Engineering*, 5th ed., Wiley, Hoboken, New Jersey (2008).